JSER

Journal of Solar Energy Research (JSER)

Journal homepage: www.jser.ut.ac.ir

Thermodynamic and exergoeconomic analyses of a solar based energy system for the provision of heating, electricity and fresh water

S. Samadzadeh Baghani[a,*], A.R. Raoufpanah[a], E. Gholamian[b]

[a] *School of Mechanical engineering, Islamic Azad University, Yadegare Emam Branch, Tehram Iran, *Email: saeed.samadzadeh.ba@gmail.com*

[b] *School of Mechanical engineering, university of Tehran, Tehram, Iran*

ARTICLE INFO

Received: 25 May 2018
Received in revised form: 15 June 2018
Accepted: 1 Aug 2018
Available online: 7 Aug 2018

Keywords:
PVT, RO, diesel engine, ORC, exergoeconomic

A B S T R A C T

The aim of this paper is to propose a solar based energy system for the provision of heating, electricity and fresh water. The proposed system in this study consists of four main parts: a geothermal based Organic Rankine cycle, a diesel engine, PVT panels and reverse osmosis desalination unit. The system is comprehensively studied from energy, exergy and exergoeconomic viewpoints. Accordingly, parametric study is performed to examine the influence of the effective parameters on the performance and economic indicators and also on the fresh water production. The results show that, by increasing the turbine inlet pressure, the fresh water prodcution rate would increase by 1.3 ton/day. Moreover, increasing the turbine inlet pressure can increase the total power output by around 800 kW. The exergoeconomic results indicate that increasing the mass flow rate of the geothermal brine increases the total cost rate by 200 $/h.

1. Introduction

Designing and investigating new multi-generation plants has been extensively studied for various perspectives. Moreover, integration of the desalination units are among the hot research topics in recent years. In the past decades, many researchers tried to examine Organic Rankine cycles because of their clear advantages.

Braimakis and Karellas [1] proposed and examined some new concepts of ORC. Yang et al. [2] investigated the integration of ORC with diesel engine. They tried to exploit the waste heat of the diesel engine in the ORC cycle. Aali et al. [3], examined different working fluids of ORC on Sabalan power plant. The results show that R141b would be the most suitable fluid and the product cost and exergy efficiency is 4.901 $/GJ and 52.56%. Xi et al. [4] proposed different concepts of ORC cycle and tried to optimize the systems. The results reveal that the double-stage cycle is more suitable model. Wang et al. [5], investigated low temperature brines on the performance of the ORC system. Assuming isobutane as the working fluid, 49.88 kW power generation is expected. Zare [6] compared the performance of the different ORC concepts from exergy and economic stand points. The results show that basic ORC would be more suitable system from economic viewpoint. Among all kind of renewable energy resources solar energy is the most abundant source and the cleanest one for the environment. Photovoltaic/thermal (PVT) is a promising technology for converting solar energy into electricity. Cooling the cells or reducing the cells temperature can enhance the performance of the PVT panels [7]. Recovering the waste heat of the PVT panels can definitely decrease the cell's temperature and hence increase the performance of the panels [8]. Gaur and Tiwari [9] examined the effect of the cell's temperature on the performance of the PVT panels. The results indicate that the thermal efficiency of PVT panels with and without cooling unit would be 7.36% and 6.85%, respectively. Notton et al. [10] showed that the physical and meteorological variables can directly affect the temperature and subsequently the performance of the PVT panels.

In addition, many researchers tried to propose new integrated energy system consisting of the RO units. Salcedo et al. [11] proposed integration of a Rankine cycle with RO unit. Nemati [12] designed the integration of Rankine cycle with engine and RO desalination system. Monnot et al. [13] proposed small RO desalination system combined with PVT panels and Manolakos et al. [14] investigated Rankine based system combined with RO unit.

According to the comprehensive literature survey, the scientific literature lacks about energy, exergy and exergoeconomic assessment of an integrated energy system consisting of a geothermal based ORC, PVT panels, RO desalination unit, and a diesel engine. The proposed integrated energy system is comprehensively modeled and examined from various thermodynamic viewpoints. The proposed integration is a promising method for the province of electricity, heating and fresh water.

2. System description and assumptions

Proposed energy system is illustrated in Fig. 1. As the figure indicates, the system has four main parts: A geothermal based ORC, a desalination unit, PVT panels and a diesel engine. PVT panels, diesel engine along with geothermal based ORC are established for power generation. Diesel engine and PVT panels are also employed for heating demand. RO desalination unit is established for preparing fresh water by using PVT panel, diesel engine and 50% of the ORC power output.
As the figure depicts, in the proposed system geothermal brine heats up the ORC working fluid by means of an evaporator and the superheater. The fluid then passes through the turbine at state 4 and thereafter is cooled down by passing on the condenser at state 5. Cooled down fluid is yet pumped again to the evaporator by means of a pump (states 1 and 2).

On the other hand, salty water enters the desalination unit by means of a suction pump (state13). In this state, reverse osmosis plant prepare fresh water by using PVT panels, diesel engine and 50% of ORC turbine power output. PVT panels and diesel engine heat up the fresh water and hot water can be used in the factory.
Following assumptions are made in this work to model the considered system:

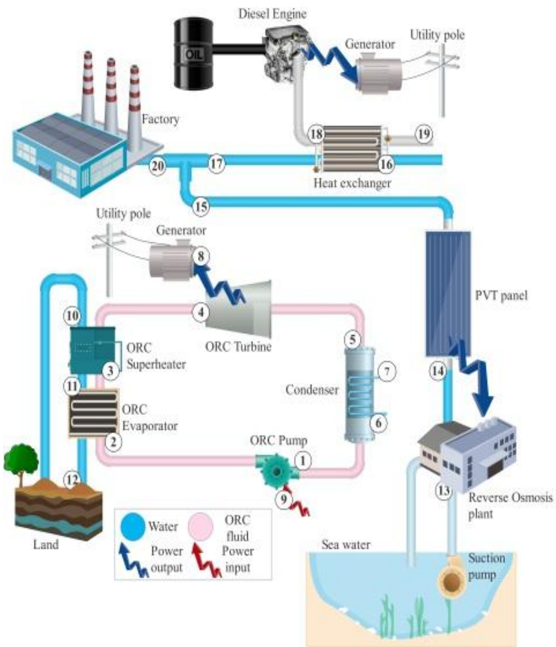

Figure 1. Schematic of the proposed energy system

- The system operates at steady state condition.
- Potential and kinetic energy changes are omitted.
- Pressure drop inside the piping system is ignored.
- Pumps and the turbine are presumed as adiabatic equipment.
- Saturated fluid is considered for the geothermal brine.

3. Modelling

Modeling and analyses of the system are performed considering energy and exergy balance for the components. Modelling of each component is described in this section.

3.1 PVT panels

The amount of absorbed solar heat by the PVT panels can be expressed as [15]:

$$\dot{Q}_{PVT} = A\eta_{opt} \quad (1)$$

where η_{opt} is the optimal efficiency and A is the area of PVT panels.

The amount of power output of the PVT panels can be defined as [15]:

$$\dot{W}_{PVT} = \dot{Q}_{PVT}\eta_{PVT}\eta_{inv} \quad (2)$$

By writing the energy equation for the PVT panels, following equation will be obtained for calculating the useful heat rate of PVT panels:

$$\dot{Q}_{useful} = \dot{Q}_{PVT} + \dot{Q}_{rad} + \dot{Q}_{conv} \quad (3)$$

In Eq. (3), useful heat rate can be written as [15]:

$$\dot{Q}_{useful} = \dot{Q}_{PVT}\left(1-\eta_{PVT}\right) \quad (4)$$

Moreover, convection and radiation heat losses can be written as:

$$\dot{Q}_{conv} = hA\left(T_{gl}-T_a\right) + hA\left(T_{ins}-T_a\right) \quad (5)$$

$$\dot{Q}_{rad} = \sigma\varepsilon A\left(\left(T_{gl}^4-T_a^4\right)+\left(T_{ins}^4-T_{sky}^4\right)\right) \quad (6)$$

where sky temperature is defined as [16]:

$$T_{sky} = 0.0522T_a^{1.5} \quad (7)$$

In Eq. (2) PVT panels' efficiency could be expressed as [15]:

$$\eta_{PVT} = \eta_{ref}\left(1-\beta_{ref}\left(T_c-T_{ref}\right)\right) \quad (8)$$

Additionally, following equation is used to predict the convection heat loss coefficient [17]:

$$h = 2.8 + 3V_{wind} \quad (9)$$

3.2 Diesel engine

Fuel feeding rate of the diesel engine is defined as [18]:

$$\dot{m}_{fuel} = 0.167\dot{W}_{diesel} \quad (10)$$

where $\dot{m}_{fuel}$ is in kg/h.

According to the assumptions of Ref. [19], the composition of the off-gases of the diesel engine is considered as 15.1% CO_2, 5.37% H_2O, 73.04% N_2 and 6.49% O_2. Exhaust gas temperature is equal to 519 °C and off-gases mass flow rate is assumed to be 19 times higher than fuel consumption.

3.3 RO desalination unit

For the RO desalination unit, net work input rate is expressible as [17]:

$$\dot{W}_{net,RO} = b_n(\dot{W}_{pump,RO} - \dot{W}_{turbine,RO}) \quad (11)$$

where, b_n is the number of trains, (7 in this study). Required work for turbine and pump of the desalination unit are expressible as [17]:

$$\dot{W}_{pump,RO} = \frac{\Delta P\dot{m}_{13}}{\eta_{pump}\rho_{13}} \quad (12)$$

$$\dot{W}_{turbine,RO} = \frac{\Delta P\dot{m}_{13}\eta_{turbine}}{\rho_{13}} \quad (13)$$

where ΔP is the transmembrane pressure, and η_{pump} and $\eta_{turbine}$ are RO pump and hydro-turbine isentropic efficiencies respectively. The target fresh water mass flow rate, $\dot{m}_{14}$, is determined from the electricity driving the RO unit and the recovery ratio *RR*, which is one of the technical characteristics of the membrane, as follows:

$$\dot{m}_{13} = \frac{\dot{m}_{14}}{RR} \quad (14)$$

The transmembrane pressure can be expressed by the following equation [17]:

$$\Delta P = J_w k_m + \Delta\pi \quad (15)$$

where k_m is the membrane permeability resistance, which has a value of 8.03 × 10^{-11} m^2s/kgPa ,and J_w is the volumetric permeate flow rate, expressed as [17]:

$$J_w = \frac{\dot{m}_{14}}{\rho_{14}nA_{mem}} \quad (16)$$

Here, *n* is the total number of membranes, which is 600 in this analysis, ρ_{14} is the density at point 14 and A_{mem} is the membrane area. In Eq. 15, $\Delta\pi$ is the transmembrane osmotic pressure, which can be expressed as follows [17]:

$$\Delta\pi = 805.1\times10^5 C_w R \quad (17)$$

Here, C_w is the membrane wall concentration, which can be expressed as [17]:

$$C_w = \frac{e^{\left(\frac{j_w}{k_{mass}}\right)}X_{13}}{e^{\left(\frac{j_w}{k_{mass}}\right)}\left(1-R\right)+R} \quad (18)$$

where *X* is the salt/water mass ratio and *R* denotes the membrane rejection coefficient, which has a value of 0.9975 in this analysis based on Ahmadi et al. [17] Also, K_{mass} is the mass transfer coefficient, expressed as follows [17]:

$$K_{mass} = 0.04\times\mathrm{Re}^{0.75}Sc^{0.33}\frac{D_s}{d} \quad (19)$$

where D_s is the diffusivity and *d* is the feed channel thickness (0.71 mm) in this analysis.

Furthermore, the Reynolds number could be expressed as [17]:

$$\mathrm{Re}_{13} = \frac{\dot{m}_{13}}{N_{ch}L_w\mu_{13}N_p} \quad (20)$$

where N_{ch} and N_P represent the number of feed channels and the number of pressure vessels respectively, μ_{13} is the dynamic viscosity of the water, and L_W is the membrane width. Also, in Eq. 19, *Sc* is the Schmidt number, defined as:

$$Sc = \frac{\mu_{13}}{\rho_{13}D_s} \quad (21)$$

3.4 ORC cycle

ORC components have been modelled based on energy balance equations.

For the turbine we have:

$$\eta_t = \frac{h_4-h_5}{h_4-h_{5s}}, \dot{W}_t = \dot{m}_1\left(h_4-h_5\right) \quad (22)$$

And for modelling the pump:

$$\eta_p = \frac{v_1(P_2 - P_1)}{h_2 - h_1}, \dot{W}_p = \dot{m}_1(h_2 - h_1) \quad (23)$$

For the evaporator and superheater we have:

$$\dot{Q}_{ev} = \dot{m}_1(h_3 - h_2) = \dot{m}_{10}(h_{11} - h_{12}) \quad (24)$$

$$\dot{Q}_{\sup} = \dot{m}_1(h_4 - h_3) = \dot{m}_{10}(h_{10} - h_{11}) \quad (25)$$

Eventually, for the condenser following equation is used:

$$\dot{Q}_{cond} = \dot{m}_1(h_5 - h_1) = \dot{m}_6(h_7 - h_6) \quad (26)$$

4. Performance examination

For investigating the performance and economic aspects of the systems, exergy efficiency, total cost rate, total power output (power of turbine, PVT and diesel) and fresh water production rate are analysed. Noteworthy, net power output of the system would be 50% of the turbine since power output of diesel and PVT panels and also half of turbine generation are transferred in RO unit. Following equations are used to examine the performance of the system:

$$\eta_{II} = \frac{\dot{W}_t - \dot{W}_p + \dot{W}_{diesel} + \dot{W}_{PVT} + \dot{E}_{heating} + \dot{E}_{14} - \dot{W}_{net,RO}}{\dot{E}_6 + \dot{E}_{fuel}} \quad (27)$$

$$\dot{C}_{tot} = \sum \dot{Z}_k + \dot{C}_{fuel} \quad (28)$$

$$\dot{Q}_{heating} = \dot{Q}_{useful,PVT} + \dot{Q}_{diesel} \quad (29)$$

In Eq. 27, Ė is the exergy rate and is expressed as:

$$\dot{E}_i = \dot{m}_i\left(h_i - h_0 - T_0(s_i - s_0)\right) \quad (30)$$

Moreover, $\dot{E}_{fuel}$, is the fuel exergy rate that can be found in the literature.

In Eq. 28, Ċ is the cost rate and $\dot{Z}$ is cost rate of the components that is defined as [17]:

$$\dot{Z} = \left(\frac{CRF\phi}{\tau}\right) \quad (31)$$

where, CRF is capital recovery factor and τ is annual operating years of the plant. ϕ is the operating and maintenance factor. CRF is defined as [17]:

$$CRF = \frac{i_r(1+i_r)^n}{(1+i_r)^n - 1} \quad (32)$$

where, i_r is the interest rate and n is operating years of the plant.

5. Results and discussion

Parametric study is performed to examine the influence of the effective parameters on the system. Moreover, verification of the components is provided.

5.1 Verification

In order to verify the simulation results of the ORC, a comparison is made between the results obtained in this work with those reported in literature [20,21], as outlined in Table 1, which indicates a good agreement. Kosmadakis et al. [15] for verification of PVT modelling. According to Table 2, there is a decent agreement between the results.

Table 1. Verification of ORC unit

Parameter	Literature [20,21]	Present work
Net power output (kW)	48.57	48.71
Energy efficiency (%)	12.6	12.72
Exergy efficiency (%)	46.8	47.67

Table 2: Verification of the heat recovery of PVT panels in kW

Concentration ratio	Simulated by Kosmadakis *et al.* [15]	Present simulation
2	0.513	0.495
5	2.867	2.76
10	6.791	6.92
15	10.72	10.85
20	14.64	14.92

5.2 Parametric study

Input parameters for modelling the system are listed in Table 3.

Table 3: Input variable for simulation purpose

ORC cycle		PVT panels	
T_0 (°C)	15	Parameter	Value
P_0 (bar)	1.013	η_{opt}	0.9
T_{10} (°C)	200	η_{inv}	0.9
$\dot{m}_{10}$ (kg/s)	10	η_{ref}	0.12
η_p	0.9	B_{ref}	0.004
η_t	0.85	T_{ref}	25 °C
P_4 (bar)	20	T_{air}	25 °C
ΔT_{sup}	20	T_{gl}	25 °C
$\Delta T_{p,p}$	5	T_{ins}	30 °C
CETD	5	T_{PVT}	100 °C
RO unit		Diesel Engine	
RR	0.5	T_{out} (°C)	520
b	7	LHV_{fuel} (kJ/kg)	43440
X_{13}	0.035	$\dot{m}_{fuel}$ (kg/h)	36

Moreover the cost equations of the components are listed in Table 4.

Table 4: Cost equations of the components [17]

Component	Cost equation (Z_k, $)
ORC Pump	$3540 \times \dot{W}_p^{0.71}$
ORC Turbine	$4750 \times \dot{W}_t^{0.75}$
ORC Evaporator	$309.14 \times A_{ev}^{0.85}$

ORC Condenser	$516.62\times A_{cond}^{0.6}$
PVT panels	$1000\times A_{PVT}$
RO unit	$0.98\times(3600\times \dot{m}_{14})^3$
n=20 years, τ=8000 hr, i_r=0.12, ϕ=1.06	

Effect of the PVT panels' area is examined in Fig. 2. As the figure shows, by increasing the area, the amount of heat absorption increases which leads to a clear increase in exergy efficiency and total cost rate. The amount of increment is not considerable as the panels are relatively small with 5 m^2 area. Higher values of area is useless because more heat rate increase the temperature of fresh water which can evaporate the water and is not favorable.

The figure further indicates that raising the area from 1 to 10 m^2, increases the amount of fresh water production and also heating rate. This is justified because higher area of PVT panels means higher amount of PVT power and useful heat production. Increasing the PVT area from 1 to 10 m^2 would increase the heat rate by 6 kW.

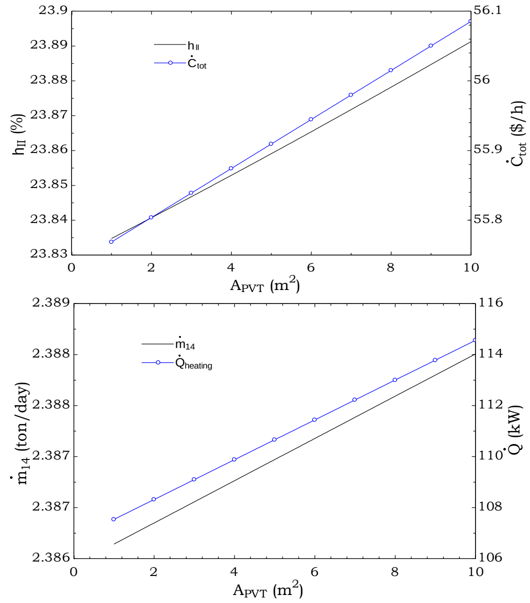

Figure 2. Effect of the PVT' area on performance and economic indicators of the system

Moreover, influence of the super heater temperature difference is depicted in Fig. 3. As the figure reveals, by increasing the parameter, total cost rate and exergy efficiency of the system drop as turbine power output decreases. The figure further shows that by raising the parameter, total output work along with fresh water production decrease.

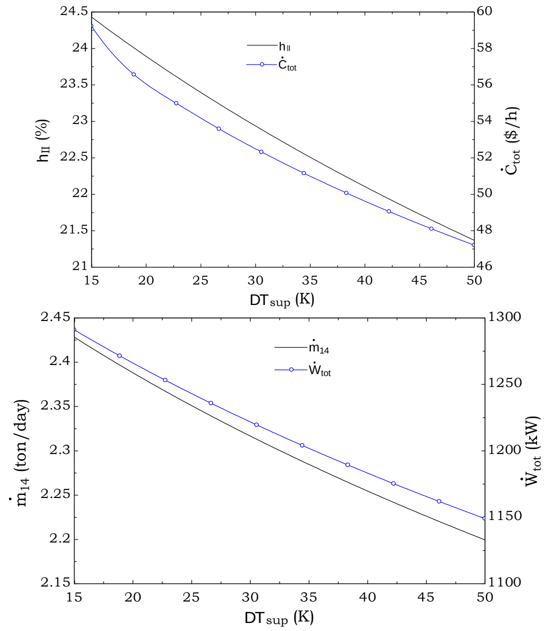

Figure 3. Effect of the superheater temperature difference on performance and economic indicators of the system

Fig. 4 shows that during shining days with higher solar radiation, the system operates efficiently with higher exergy efficiency and heating rate. This can be described because higher solar radiation raises the power output of PVT panels and also increase the heat rate of the system.

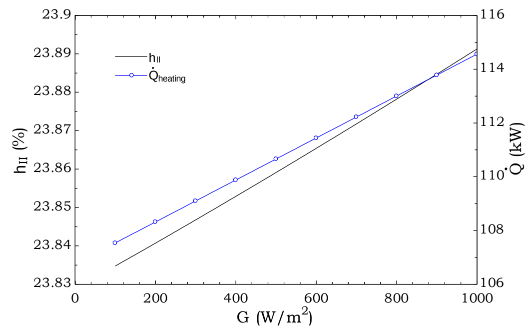

Figure 4. Effect of solar radiation on performance and economic indicators of the system

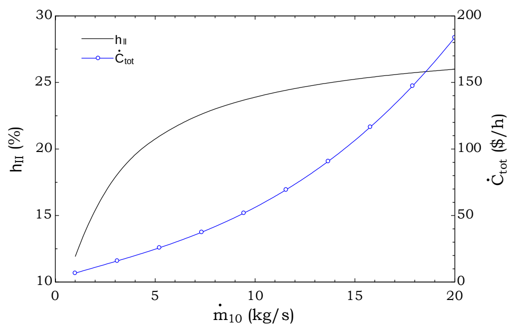

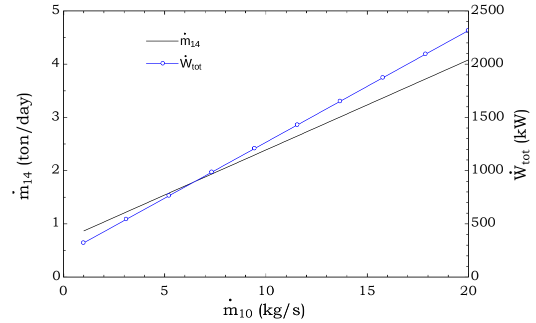

Figure 5. Effect of geothermal brine's mass flow rate on performance and economic indicators of the system

Fig. 6 presents the effect of the heat source temperature on the performance of the system. As the figure shows, higher heat source temperature can help the system to operate effectively but in the other hand total cost rate would increase. Higher heat source temperature increases the power generation of the ORC cycle which could increase the total cost rate of the turbine and or other components.

Moreover, inference from the bottom of the graph is that, increasing the geothermal brine's temperature increases the total output work and fresh water production rate. This is justified because higher heat source temperature means higher available enthalpy for the evaporator and then higher power generation of the turbine. As 50% of the power output of the turbine is transferred in the OR desalination unit, higher heat source temperature can increase the fresh water production rate.

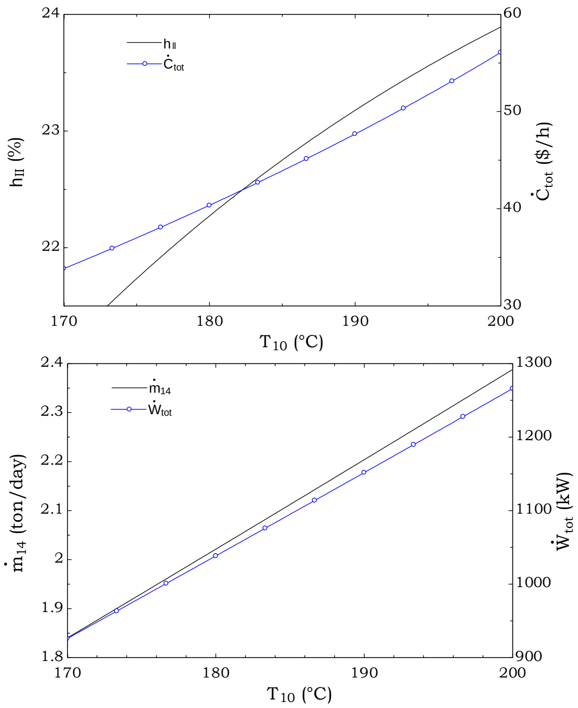

Figure 6. Effect of geothermal brine's temperature on performance and economic indicators of the system

Effect of the fuel feeding rate of the diesel engine is examined in Fig. 7. As the figure demonstrates by raising the fuel feeding rate, exergy efficiency decreases, while heating rate and total cost rate of the system increase dramatically. This can be justified because higher fuel feeding rate increase the inlet exergy and cost rate of diesel engine which can decrease the exergy efficiency and total cost rate of the system.

As the power of the diesel engine is used in RO desalination unit, higher fuel feeding rate can increase the fresh water production rate and total power output of the system.

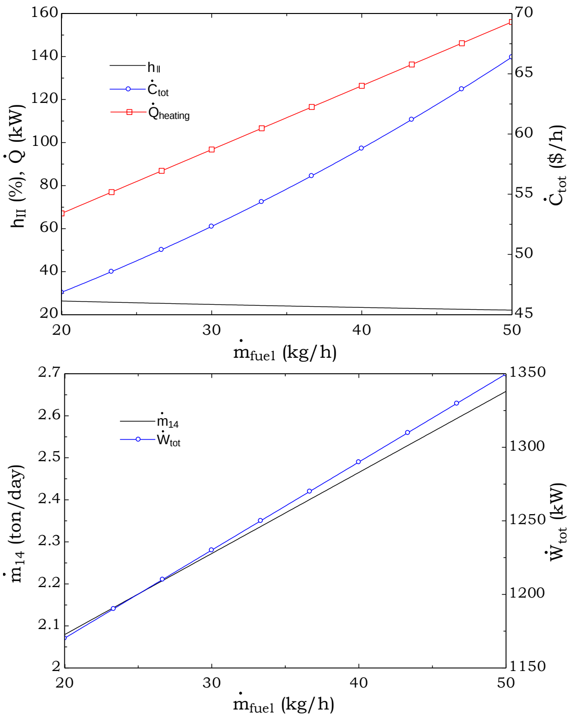

Figure 7. Effect of the fuel feeding rate of diesel engine on performance and economic indicators of the system

Last but not least effective parameter is the turbine inlet pressure. As the Fig. 8 shows, by increasing the turbine inlet pressure, the exergy efficiency and total cost rate of the system increase. In this regard, higher inlet pressure of the turbine leads to higher power generation of the turbine. As the half of the turbine's power output is used in RO desalination unit, higher fresh water production is expected in higher turbine inlet pressures.

Increasing the turbine inlet pressure can considerably increase the exergetic efficiency by 15% and also total output work by around 800 kW. Moreover, increasing the turbine inlet pressure increases the fresh water production rate by 1.3 ton/day. Accordingly, turbine inlet pressure is among the highly effective parameters and should properly selected to help the system operate effective and affordable.

6. Conclusion

In this study, a novel integrated energy system is proposed consisting of photovoltaic/thermal (PVT) panels, geothermal based Organic Rankine (ORC) cycle, diesel engine and an Reverse osmosis (RO) desalination unit for the province of the heating, electricity and fresh water. The proposed system is comprehensively modeled and examined from exergy, energy and exergoeconomic viewpoints. The results show that, by increasing the turbine inlet pressure, the fresh water prodcution rate would increase by 1.3 ton/day.

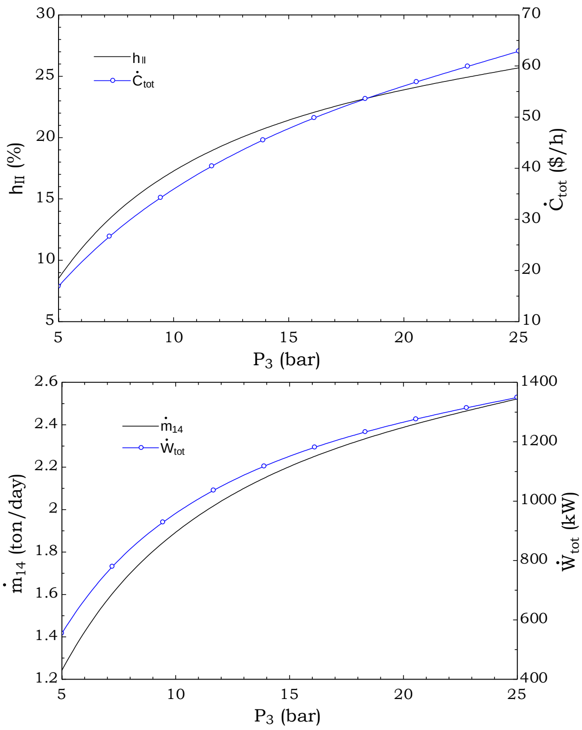

Figure 8. Effect of the turbine inlet pressure on performance and economic indicators of the system

Moreover, increasing the turbine inlet pressure can increase the total power output by around 800 kW. The exergoeconomic results indicate that increasing the mass flow rate of the geothermal brine increases the total cost rate by 200 $/h. The results further indicate that increasing the fuel feeding rate of the diesel engine increases the fresh water prodcution rate and total cost rate of the system by 0.5 ton/day and 20 $/h, respectively. Eventually, it can be concluded that the propsed integrated energy system is a promising method for the provision of electricity, heating and fresh water.

Nomenclature:	
A	Area
$\dot{C}$	Cost rate
CRF	Capital recovery factor
CETD	Cold end temperature difference
$\dot{E}$	Exergy rate
G	Solar radiation
h	Enthalpy
i_r	Interest rate
$\dot{m}$	Mass flow rate
P	Pressure
Q	Heat rate
RR	Rejection rate
s	Entropy
T	Temperature
$\dot{W}$	Work
X	Salt mass fraction
$\dot{Z}$	Cost rate of the components
Greek letters	
η	Efficiency
ρ	Density
τ	Annual operation hours
μ	Viscosity
ε	Emissivity
σ	Stefan-Boltzmann constant
ϕ	Operating and maintenance factor
Subscripts	
1, 2 ,…	State point
cond	Condenser
ev	Evaporator
p	Pump
p.p	Pinch point
sup	Superheater
t	Turbine

References

[1] Braimakis K, Karellas S. Energetic optimization of regenerative Organic Rankine Cycle (ORC) configurations. Energy Convers Manag 2018;159:353–70. doi:10.1016/j.enconman.2017.12.093.

[2] Yang F, Zhang H, Bei C, Song S, Wang E. Parametric optimization and performance analysis of ORC (organic Rankine cycle) for diesel engine waste heat recovery with a fin-and-tube evaporator. Energy 2015;91:128–41. doi:10.1016/j.energy.2015.08.034.

[3] Aali A, Pourmahmoud N, Zare V. Exergoeconomic analysis and multi-objective optimization of a novel combined flash-binary cycle for Sabalan geothermal power plant in Iran. Energy Convers Manag 2017;143:377–90. doi:10.1016/j.enconman.2017.04.025.

[4] Xi H, Li MJ, Xu C, He YL. Parametric optimization of regenerative organic Rankine cycle (ORC) for low grade waste heat recovery using genetic algorithm. Energy 2013;58:473–82. doi:10.1016/j.energy.2013.06.039.

[5] Wang J, Yan Z, Wang M, Ma S, Dai Y. Thermodynamic analysis and optimization of an (organic Rankine cycle) ORC using low grade heat source. Energy 2013;49:356–65. doi:10.1016/j.energy.2012.11.009.
[6] Zare V. A comparative exergoeconomic analysis of different ORC configurations for binary geothermal power plants. Energy Convers Manag 2015;105:127–38. doi:10.1016/j.enconman.2015.07.073.
[7] Khanjari Y, Kasaeian AB, Pourfayaz F. Evaluating the environmental parameters affecting the performance of photovoltaic thermal system using nanofluid. Appl Therm Eng 2017;115:178–87. doi:10.1016/j.applthermaleng.2016.12.104.
[8] Hazi A, Hazi G, Grigore R, Vernica S. Opportunity to use PVT systems for water heating in industry. Appl Therm Eng 2014;63:151–7. doi:10.1016/j.applthermaleng.2013.11.010.
[9] Gaur A, Tiwari GN. Performance of a-Si thin film PV modules with and without water flow: An experimental validation. Appl Energy 2014;128:184–91. doi:10.1016/j.apenergy.2014.04.070.
[10] Notton G, Cristofari C, Mattei M, Poggi P. Modelling of a double-glass photovoltaic module using finite differences. Appl Therm Eng 2005;25:2854–77. doi:10.1016/j.applthermaleng.2005.02.008.
[11] Salcedo R, Antipova E, Boer D, Jiménez L, Guillén-gosálbez G. Multi-objective optimization of solar Rankine cycles coupled with reverse osmosis desalination considering economic and life cycle environmental concerns. DES 2012;286:358–71. doi:10.1016/j.desal.2011.11.050.
[12] Nemati A, Sadeghi M, Yari M. Exergoeconomic analysis and multi-objective optimization of a marine engine waste heat driven RO desalination system integrated with an organic Rankine cycle using zeotropic working fl uid. Desalination 2017;422:113–23. doi:10.1016/j.desal.2017.08.012.
[13] Monnot M, Darío G, Carvajal M, Laborie S. Integrated approach in eco-design strategy for small RO desalination plants powered by photovoltaic energy G RA P H I C A L AB S T R A C T. Desalination 2018;435:246–58. doi:10.1016/j.desal.2017.05.015.
[14] Manolakos D, Sh E, Karagiannis I, Papadakis G. Technical and economic comparison between PV-RO system and RO-Solar Rankine system . Case study: Thirasia island 2008;221:37–46. doi:10.1016/j.desal.2007.01.066.
[15] Kosmadakis G, Manolakos D, Papadakis G. Simulation and economic analysis of a CPV / thermal system coupled with an organic Rankine cycle for increased power generation 2011;85:308–24. doi:10.1016/j.solener.2010.11.019.
[16] Habibollahzade A, Houshfar E, Ashjaee M, Behzadi A, Gholamian E, Mehdizadeh H. Enhanced power generation through integrated renewable energy plants: Solar chimney and waste-to-energy. Energy Convers Manag 2018;166:48–63. doi:10.1016/j.enconman.2018.04.010.
[17] Dinçer I, Rosen M, Ahmadi P. Optimization of energy systems. John Wiley & Sons; 2017.
[18] Yang M. Payback period investigation of the organic Rankine cycle with mixed working fl uids to recover waste heat from the exhaust gas of a large marine diesel engine. Energy Convers Manag 2018;162:189–202. doi:10.1016/j.enconman.2018.02.032.
[19] Radulovic J, Benedikt K. Utilisation of diesel engine waste heat by Organic Rankine Cycle 2015;78:437–48. doi:10.1016/j.applthermaleng.2015.01.004.
[20] Ogriseck S. Integration of Kalina cycle in a combined heat and power plant, a case study. Appl Therm Eng 2009;29:2843–8. doi:https://doi.org/10.1016/j.applthermaleng.2009.02.006.
[21] Yari M. Exergetic analysis of various types of geothermal power plants. Renew Energy 2010;35:112–21. doi:10.1016/j.renene.2009.07.023.